Coregulator Sin3a Promotes Postnatal Murine β-Cell Fitness by Regulating Genes in Ca^{2+} Homeostasis, Cell Survival, Vesicle Biosynthesis, Glucose Metabolism, and Stress Response

Xiaodun Yang,[1] Sarah M. Graff,[2] Cody N. Heiser,[1,3,4] Kung-Hsien Ho,[1] Bob Chen,[1,3,4] Alan J. Simmons,[1,3] Austin N. Southard-Smith,[1,3] Gregory David,[5] David A. Jacobson,[2] Irina Kaverina,[1] Christopher V.E. Wright,[1] Ken S. Lau,[1,3,4] and Guoqiang Gu[1]

Diabetes 2020;69:1219–1231 | https://doi.org/10.2337/db19-0721

Swi-independent 3a and 3b (Sin3a and Sin3b) are paralogous transcriptional coregulators that direct cellular differentiation, survival, and function. Here, we report that mouse Sin3a and Sin3b are coproduced in most pancreatic cells during embryogenesis but become much more enriched in endocrine cells in adults, implying continued essential roles in mature endocrine cell function. Mice with loss of *Sin3a* in endocrine progenitors were normal during early postnatal stages but gradually developed diabetes before weaning. These physiological defects were preceded by the compromised survival, insulin-vesicle packaging, insulin secretion, and nutrient-induced Ca^{2+} influx of *Sin3a*-deficient β-cells. RNA sequencing coupled with candidate chromatin immunoprecipitation assays revealed several genes that could be directly regulated by Sin3a in β-cells, which modulate Ca^{2+}/ion transport, cell survival, vesicle/membrane trafficking, glucose metabolism, and stress responses. Finally, mice with loss of both *Sin3a* and *Sin3b* in multipotent embryonic pancreatic progenitors had significantly reduced islet cell mass at birth, caused by decreased endocrine progenitor production and increased β-cell death. These findings highlight the stage-specific requirements for the presumed "general" coregulators Sin3a and Sin3b in islet β-cells, with Sin3a being dispensable for differentiation but required for postnatal function and survival.

Islet β-cell differentiation starts during early embryogenesis when a subset of pancreatic multipotent progenitor cells (MPCs) activates the expression of transcription factor (TF) neurogenin 3 (*Ngn3* or *Neurog3*) and subsequently dozens of other islet cell TFs (1). During perinatal growth, the differentiated β-cells proliferate to increase their overall mass while also fine-tuning gene expression profiles to become mature, functional cells (2). Besides TFs, several transcriptional coregulators, including the mixed-lineage leukemia 3 and 4 methyltransferases (3) and Swi/Snf complexes (4), are essential for the production and/or maturation of β-cells. The standard model is that specific combinations of coregulators and TFs organize the chromatin landscape to shape the transcriptomic profiles of progenitors for cell development and function (4).

Swi-independent 3 (Sin3) is a well-established coregulator conserved from yeast to human cells (5). It does not bind DNA but uses several highly conserved amphipathic α-helices to interact with a variety of TFs and other coregulators, including P53, Mad1, Myc, REST, and ESET (5,6). In addition, Sin3 contains binding sites for histone

[1]Vanderbilt Program in Developmental Biology, Vanderbilt Center for Stem Cell Biology, Department of Cell and Developmental Biology, Vanderbilt University School of Medicine, Nashville, TN
[2]Department of Molecular Physiology and Biophysics, Vanderbilt University School of Medicine, Nashville, TN
[3]Epithelial Biology Center, Vanderbilt Medical Center, Nashville, TN
[4]Program in Chemical and Physical Biology, Vanderbilt University School of Medicine, Nashville, TN
[5]Department of Biochemistry and Molecular Pharmacology, New York University, New York, NY

Corresponding author: Guoqiang Gu, guoqiang.gu@vanderbilt.edu

Received 22 July 2019 and accepted 26 March 2020

This article contains supplementary material online: https://doi.org/10.2337/db20-4567/suppl.12042828.

deacetylases, histone lysine methylases, and demethylases (7–9). Thus, Sin3 primarily acts as a scaffold protein to assemble chromatin-modifying complexes that regulate gene transcription, and its target gene selectivity is determined by the DNA-binding TFs that recruit Sin3 (7–9). Notably, although Sin3 was commonly known as a "corepressor," several studies suggest that it can coactivate gene expression in some cellular contexts (10).

Sin3 has two paralogs in mammalian cells, *Sin3a* and *Sin3b*, with evidence showing overlapping yet distinct functions (5,10). In mice, *Sin3a*, but not *Sin3b*, is essential in cell survival and/or differentiation during embryogenesis. Nullizygous $Sin3a^{-/-}$ mouse embryos died shortly after implantation, whereas *Sin3b*-null mice were born with seemingly normal organs but died immediately after birth (5). Consequently, *Sin3a* was reported to be required for the development and/or survival of embryonic stem (ES) cells (11,12), muscle cells (13), male germ cells (14), lung progenitors (15), and some skin cells (16). In addition, gene expression and protein-DNA interaction studies showed that Sin3a could directly regulate molecules involved in cell proliferation, survival, metabolism, and stress responses (7,17,18), yet how Sin3a functions in postnatal organs has not been examined.

In pancreatic cells, Sin3a was detected in transcriptional complexes containing Myt, Mafa, and/or Foxo TFs, which are all required for β-cell function (3,19,20). In this study, we assessed the roles and mechanisms of *Sin3*, focusing on *Sin3a*, in embryonic development and postnatal function of mouse islet β-cells. We show that *Sin3a* is dispensable for islet cell differentiation but required for β-cell function and survival, that is, their postnatal "fitness." In addition, although Sin3 activity, sufficiently provided by either Sin3a or Sin3b, is essential for endocrine specification from MPCs, it is not needed for the differentiation of endocrine progenitors into islet hormone-positive cells. Thus, our data reveal stage- and cell-type–specific roles of the Sin3 complex, with Sin3a being particularly important for postnatal β-cell fitness.

RESEARCH DESIGN AND METHODS

Mice

Mouse usage was supervised by the Vanderbilt University institutional animal care and use committee in compliance with Association for Assessment and Accreditation of Laboratory Animal Care regulations. $Sin3a^{F}$, $Sin3a^{-}$, $Sin3b^{F}$, and $Sin3b^{-}$ mice were previously described (17,21). $Pdx1^{Cre}$ [*Tg(Pdx1Cre)89.1Dam*], *Ai9* [*Cg-Gt(ROSA)26Sor*$^{tm9(CAG\text{-}tdTomato)Hze}$/J], and *Neurog3-Cre* [*Tg(Neurog3-Cre)C1Able/J*] mice were from The Jackson Laboratory. ICR (CD1) mice were from Charles River Laboratories. All analyzed mice had a mixed genetic background (~25% CD1, ~37.5% C57BL/6, and ~37.5% 129/Sv, as estimated from crossing history). The day of vaginal plug appearance was counted as embryonic day 0.5 (E0.5), and the day of birth was counted as postnatal day 1 (P1). PCR-based genotyping used oligos listed in Supplementary Table 1.

Tissue Preparation, Immunofluorescence Detection, and Imaging

Tissue preparation and immunofluorescence (IF) analysis followed routine protocols using 10-μm-thick frozen sections (19). Primary antibodies (1:500 to 1:2,000 dilution) were as follows: rabbit anti-Sin3a (LS-C331555; Lifespan Biosciences), rabbit anti-Sin3b (ab101841; Abcam), rabbit anti-Mafa (NBP1-00121; Novus Biologicals), rabbit anti-Mafb (IHC-00351; Bethyl Laboratories), rabbit anti-Nkx6.1 (gift from Palle Serup, University of Copenhagen, Copenhagen, Denmark), goat anti-Pdx1 (ab47303 [Abcam] or 06-13850 [Millipore]) (22), goat anti-Neurog3 (this laboratory, available upon request) (23), rabbit anti-Glut2 (GT21-A; Alpha Diagnostic), rabbit anti-Ucn3 (ab79121; Abcam), guinea pig anti-insulin (A0564; Dako), rabbit anti-glucagon (ab92517; Abcam), goat anti-somatostatin (sc-7819; Santa Cruz Biotechnology), rabbit anti–cleaved caspase-3 (#9661; Cell Signaling Technology), and rabbit anti-Ki67 (ab15580; Abcam). Secondary antibodies (1:500) used included the following: Alexa Fluor 488 donkey anti-guinea pig (706-545-148), Cy3 donkey anti-rabbit (711-165-152), Cy3 donkey anti-goat (705-165-147), Alexa Fluor 647 donkey anti-guinea pig (706-605-148), Alexa Fluor 647 donkey anti-rabbit (711-605-152), and Alexa Fluor 647 donkey anti-goat (705-605-147), all from Jackson ImmunoResearch.

Images were taken using a Nikon spinning disk confocal microscope and quantified with ImageJ 1.51j 14 software (National Institutes of Health [NIH]) under double-blind settings using 16-bit images. The presented results are the average intensity per pixel within the region of interest. The region of interest was manually selected to encircle the plasma membrane (for Glut2), cytoplasm (Ucn3), or nuclei (Mafa) of β-cells. We then normalized the relative levels of control cells to 1.0 for comparison. For each sample, 12–15 islet sections were examined. Transmission electron microscopy (TEM) and quantification followed published protocols (19).

Islet Cell Mass Measurement

One of every 12 sections (~120 μm apart) of entire P1 and P7 pancreata and 1 of every 18 sections (~180 μm apart) of P14 pancreata were scored. The sections were costained with DAPI and hormone antibodies to identify all cells and islet cells, respectively. Tissue sections were scanned/analyzed using Aperio ImageScope software (Leica Biosystems). The islet cell mass was calculated as follows: islet cell mass (mg) = (hormone + area / DAPI-positive area) × pancreas weight (mg).

Blood Glucose/Insulin Secretion Assays, Insulin Tolerance Test, and Intraperitoneal Glucose Tolerance Test

Blood glucose was measured through tail snipping. Plasma insulin/glucagon assays used blood from the retro-orbital collection. Islet isolation and secretion assays followed published protocol (19). Handpicked islets, after overnight recovery in RPMI medium (10% v/v FBS and 11.0 mmol/L glucose), were incubated in Krebs-Ringer buffer (KRB),

containing 2.8 mmol/L glucose, for 1 h, with 2.8 mmol/L glucose for 45 min, then in KRB with 20 mmol/L glucose for 45 min, and lastly in KRB with 25 mmol/L KCl and 2.8 mmol/L glucose for 45 min. Insulin was measured using an ELISA kit from ALPCO and glucagon with a kit from Mercodia (Uppsala, Sweden) in the Vanderbilt Hormone Assay and Analytical Services Core. Insulin tolerance test and intraperitoneal glucose tolerance test followed that in Huang et al. (19).

Ca^{2+} Imaging

Ca^{2+} imaging followed published protocols (24). P5 islets were attached to poly-lysine–coated dishes overnight in RPMI medium (10% FBS and 11.0 mmol/L glucose). Islets were incubated in RPMI medium/10% FBS/2.8 mmol/L glucose basal media with 2.0 mmol/L Fura-2 AM (Invitrogen) for 20 min, followed by 20 min of washing in basal media. Ca^{2+} imaging was performed in recording solution (119 mmol/L NaCl, 2.5 mmol/L $CaCl_2$, 4.7 mmol/L KCl, 10 mmol/L HEPES, 1.2 mmol/L $MgSO_4$, and 1.2 mmol/L KH_2PO_4). The islets were perfused at 2.0 mL/min at 37°C with 2.8 mmol/L glucose (0–195 s), 20 mmol/L glucose (196–915 s), 2.8 mmol/L glucose (916–1,800 s), and 25 mmol/L KCl with 2.8 mmol/L glucose (1,801–2,090 s). Fluorescence images, excited at 340 and 380 nm (F340/F380), were taken/measured every 5 s with a Nikon Eclipse Ti2 microscope and Photometrics Prime 95B 25mm sCMOS camera.

Quantitative RT-PCR and Single-Cell RNA Sequencing

Quantitative RT-PCR (qRT-PCR) followed routine procedures using Universal SYBR Green Supermix (Bio-Rad) on a Bio-Rad CFX96 thermal cycler. Transcript abundance was normalized to *Gapdh*. Oligos are listed in Supplementary Table 1.

For single-cell RNA sequencing (scRNA-seq), two batches of P4 $Sin3a^{F/+}$ and $Sin3a^{\Delta endo}$ islets (two to four mice of each genotype used for each batch) were isolated and dissociated into single cells using trypsin-EDTA. After live cell selection, the inDrop platform (1CellBio) was used to encapsulate and barcode single cells used for CEL-Seq–based library preparation and sequencing (NextSeq 500; Illumina). Reads were assigned to individual cells. After adaptor sequences were trimmed and cell doublets corrected, batch alignment assigned the reads to specific gene loci or unique molecular identifiers. We next identified β-cells based on *insulin 1* and *insulin 2* gene expression, which were then compared with the Mouse Cell Atlas to verify their cell identity (25). Afterward, the number of reads of each unique molecular identifier within each sample were combined and analyzed as one bulk sample using DESeq2. Log(fold change [FC]) was calculated as log(2){[(level in mutant) − (level in control)] / (level in control)}. Statistical analyses used the Wilcoxon rank sum test, and the adjusted *P* values were derived using the Bonferroni posttest correction on the basis of the total number of genes in the data set. Gene set enrichment assays (GSEAs) followed that in Subramanian et al. (26). Gene ontology–based Database for Annotation, Visualization, and Integrated Discovery analysis of potential Sin3a-binding genes followed that in Huang et al. (27).

Chromatin Immunoprecipitation Assays

A Magna ChIP-HiSens Chromatin Immunoprecipitation Kit (MilliporeSigma) was used. MIN6 cells (passage #38–43) were fixed for 20 min using 2.0 mmol/L disuccinimidyl glutarate followed by an additional 12 min with 1% formaldehyde. Sheared chromatin (200–500 bp) was prepared using a Bioruptor Pico (Diagenode) (~30 cycles of 30 s sonication + 30 s rest). For each immunoprecipitation, 2.0 μg of chromatin and 2.0 μg of antibodies were used. The normal rabbit IgG was from Cell Signaling Technology (Cat# 2729). The rabbit anti-Sin3a (LS-C331555) was from Lifespan Biosciences.

Statistics for Non-scRNA-Seq Data

SPSS version 25 statistical software (IBM Corporation) was used. Data are shown as mean ± SD. Student *t* test or one-way repeated-measures ANOVA was used to compare two groups or more than two groups of data, respectively. $P < 0.05$ was considered significant.

Data and Resource Availability

The data sets generated and/or analyzed during the current study are deposited in Gene Expression Omnibus (GEO) under GSE146474 and are freely available for all. The data are also available from the corresponding author upon reasonable request.

RESULTS

Pan-Pancreatic Sin3a/Sin3b Expression During Embryogenesis Becomes Enriched in Adult Endocrine Cells

At E10.5, E15.5, and P1, both Sin3a and Sin3b proteins were detected in most pancreatic cells (Fig. 1*A*–*C*), including $Neurog3^+$ endocrine progenitors (Fig. 1*B*) and hormone-positive islet cells (Fig. 1*C*). After P1, their expression further increased, and they became highly enriched in islet cells (Fig. 1*D* and *E*). However, both Sin3a and Sin3b remained detectable in some nonislet cells in the 3-month-old pancreas (Fig. 1*E*).

Loss of *Sin3a* Causes Late-Onset Diabetes

$Sin3a^{F/-}$; *Neurog3-Cre* mice (termed $Sin3a^{\Delta endo}$) were derived to inactivate *Sin3a* in the endocrine progenitors and some neuronal cells (28). IF and qRT-PCR assays supported the efficient deletion of *Sin3a* in $Sin3a^{\Delta endo}$ islets (Fig. 2*A* and *B*). We examined male and female $Sin3a^{F/-}$, $Sin3a^{F/+}$, and $Sin3a^{F/+}$; *Neurog3-Cre* mice. No significant differences were observed in body weight, ad lib–fed blood glucose, islet structure, or expression of several diagnostic endocrine markers (e.g., Mafa, Pdx1, Nkx6.1, hormones), except that $Sin3a^{F/-}$ female mice had slightly lower body weights compared with $Sin3a^{F/+}$ females at 2 weeks of age (Supplementary Fig. 1*A*–*F*). Thus, we used $Sin3a^{F/-}$ mice as controls for most studies unless noted.

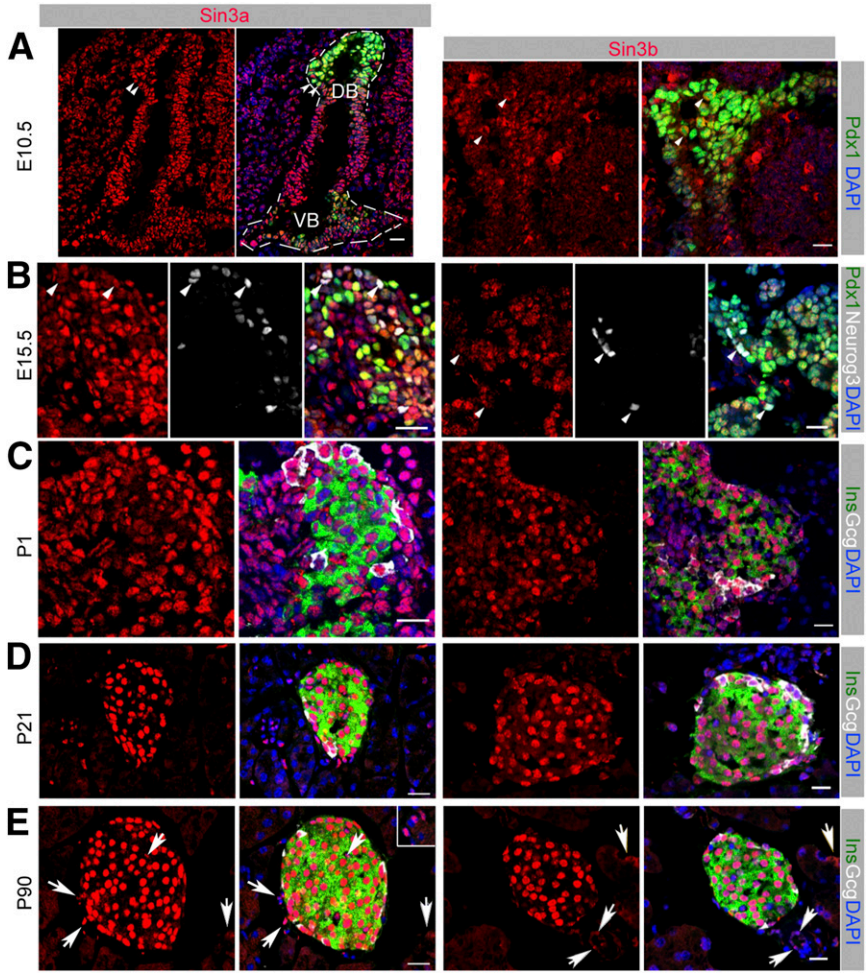

Figure 1— Sin3a and Sin3b are produced in pancreatic progenitors and islet cells. DAPI was used to mark nuclei in some panels. *A*: IF of Sin3a or Sin3b, costained with Pdx1 at E10.5. For Sin3a IF, both dorsal pancreatic bud (DB) and ventral pancreatic bud (VB) are shown. For Sin3b, only DB is shown. Arrowheads indicate Pdx1$^+$ cells that also coexpress Sin3a or Sin3b. *B*: Costaining of Sin3a/Sin3b, Neurog3, and Pdx1 at E15.5. Arrowheads indicate Neurog3$^+$ cells that also express Sin3a or Sin3b. *C–E*: IF of Sin3a, Sin3b, insulin, and glucagon in P1, P21, and P90 pancreata. Arrows in *E* point to several nonislet cells that express Sin3a or Sin3b. Scale bars = 20 μm.

Up to P14, both male and female *Sin3a*$^{\Delta endo}$ mice had body weights indistinguishable from control littermates but showed significant growth retardation afterward (Fig. 2*C*). The *Sin3a*$^{\Delta endo}$ mice showed normal glycemia at P7 but significantly higher blood glucose levels afterward (Fig. 2*D*). The temporal phenotypic development is similar in both male and female mice (Fig. 2*C* and *D*). We therefore used both sexes interchangeably and presented our findings together for the rest of the studies unless noted.

Sin3a$^{\Delta endo}$ mice had significantly higher fasting glucose levels on P28 but not on P14 (Fig. 2*E*). Compromised glucose tolerance was obvious in P14 *Sin3a*$^{\Delta endo}$ mice (Fig. 2*F*), which had normal insulin sensitivity on P14 but increased sensitivity on P21 (Fig. 2*G*). P7 and P28 *Sin3a*$^{\Delta endo}$ mice showed reduced plasma insulin (Fig. 2*H*), and plasma glucagon levels in P7 *Sin3a*$^{\Delta endo}$ mice were reduced (Fig. 2*I*). These combined findings suggest that reduced circulating insulin, but not increased glucagon or compromised insulin response, causes the hyperglycemic phenotype of *Sin3a*$^{\Delta endo}$ mice. Thus, our following studies focused on β-cells.

Sin3a Is Required for Postnatal β-Cell Function and Survival

We assayed insulin secretion of P7 *Sin3a*$^{\Delta endo}$ islets, the oldest stage when intact mutant islets could be readily isolated. These islets secreted more insulin under 2.8 mmol/L glucose (Fig. 3*A*) but less under 20 mmol/L glucose (Fig. 3*B*) or 25 mmol/L KCl (Fig. 3*C*). *Sin3a*$^{\Delta endo}$ β-cells had compromised Ca^{2+} influx induced by glucose or KCl, with higher levels of basal but a lower stimulated Ca^{2+} influx (Fig. 3*D–F*). In addition, *Sin3a*$^{\Delta endo}$ β-cells had more vesicles per unit of cytoplasmic area and a decreased size of the insulin dense core within each vesicle and more vesicle-like membrane structures that lacked detectable insulin crystals (Fig. 3*G–I*).

P7 and P14, but not P1, *Sin3a*$^{\Delta endo}$ mice had significantly reduced β-cell mass (Fig. 4*A* and *B*) accompanied by increased apoptosis starting from P1 (Fig. 4*C* and *D*)

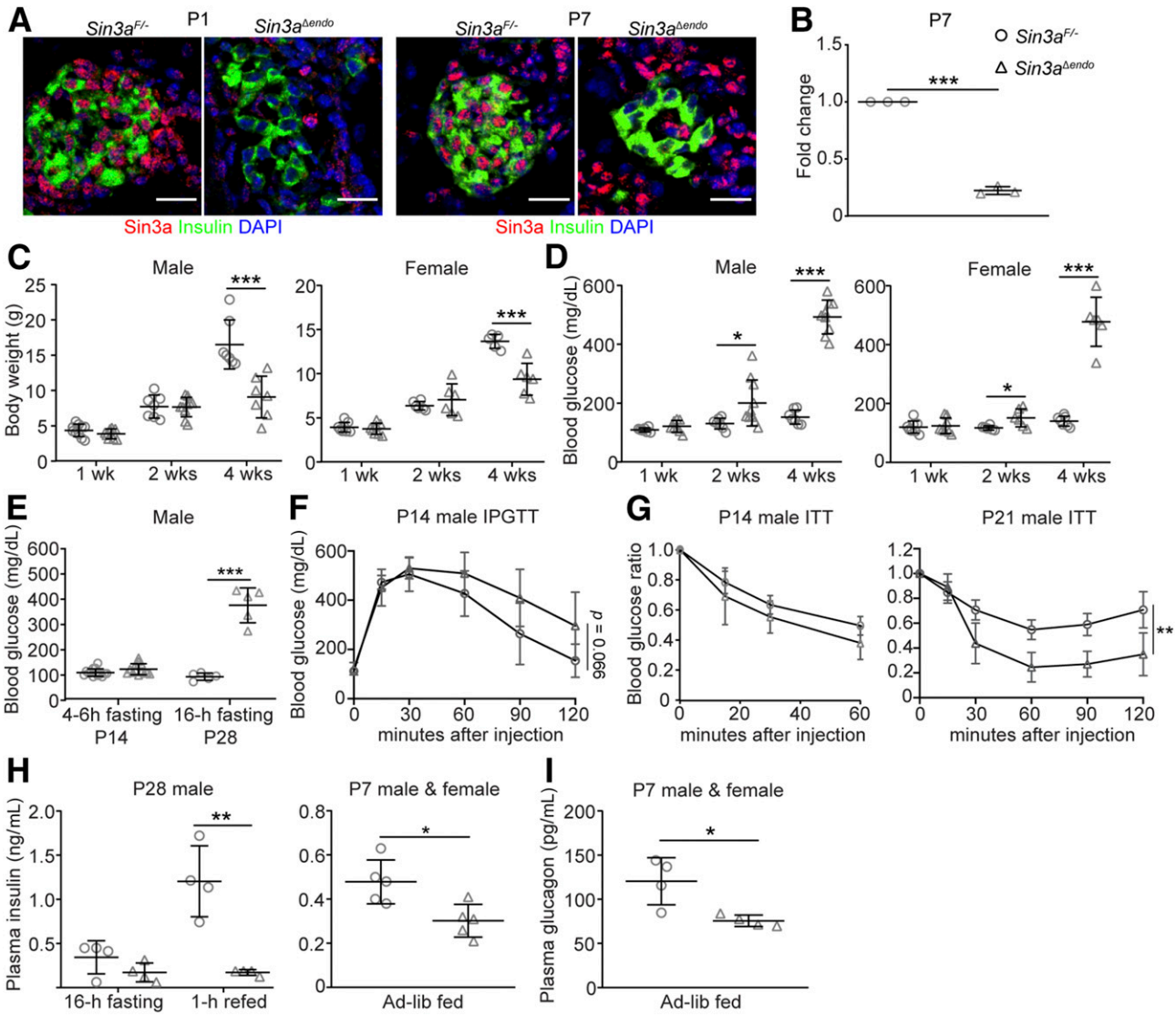

Figure 2—Loss of *Sin3a* causes late-onset diabetes. *A*: IF detection of Sin3a in P1 and P7 control and *Sin3a*$^{\Delta endo}$ pancreata, highlighting insulin-positive β-cells. DAPI counterstaining marked nuclei. Scale bars = 20 μm. *B*: RT-PCR detection of *Sin3a* transcripts in P7 control and *Sin3a*$^{\Delta endo}$ islets, amplifying the floxed exon that should be deleted. Note that the islet samples include mesenchymal and endothelial cells as well, which also express *Sin3a*. *C–I*: Phenotyping of control and *Sin3a*$^{\Delta endo}$ mice, including body weight (n = 7–10) (*C*), random-fed (n = 7–10) (*D*), or fasting (n = 5–14) (*E*) blood glucose, glucose tolerance (n = 7–8) (*F*), insulin tolerance (n = 5–6) (*G*), and plasma insulin (n = 4–5) (*H*), or glucagon (n = 4) (*I*). *$P < 0.05$, **$P < 0.01$, ***$P < 0.001$. IPGTT, intraperitoneal glucose tolerance test; ITT, insulin tolerance test; wk, week.

but no change of proliferation (Fig. 4*E* and *F*). In addition, *Sin3a*$^{\Delta endo}$ mice had reduced α-cell mass but no change in δ-cell mass in P14 (Supplementary Fig. 2). These combined findings suggest that *Sin3a* is not required for β-cell differentiation (i.e., producing insulin-positive cells) during embryogenesis but is required for their fitness after birth. This conclusion led us to examine the detailed molecular mechanisms on how Sin3a regulates this fitness.

Sin3a Regulates the Expression of Maturation and Function Genes in Postnatal β-Cells

We used a candidate approach and examined the expression of several TFs (Mafa, Mafb, Pdx1, and Nkx6.1) that are important for β-cell differentiation and maturation markers (Glut2 and Ucn3) that are important for function. Pdx1, Nkx6.1, or Mafb levels showed no difference in *Sin3a*$^{\Delta endo}$ β-cells compared with controls (Supplementary Fig. 3), but Glut2, Ucn3, and Mafa expression was progressively reduced. Specifically, Ucn3 expression was significantly downregulated by P4, while Glut2 and Mafa expression was downregulated by P7 at both protein and mRNA levels (Fig. 5 and Supplementary Fig. 4). However, because the glycemic defects of *Ucn3*- or *Mafa*-mutant mice developed much later than the *Sin3a*$^{\Delta endo}$ animals (29,30) and the increased β-cell death was observed before the downregulation of *Ucn3*, *Mafa*, and *Slc2a2*, these three genes are unlikely the major mediators of Sin3a function. Thus,

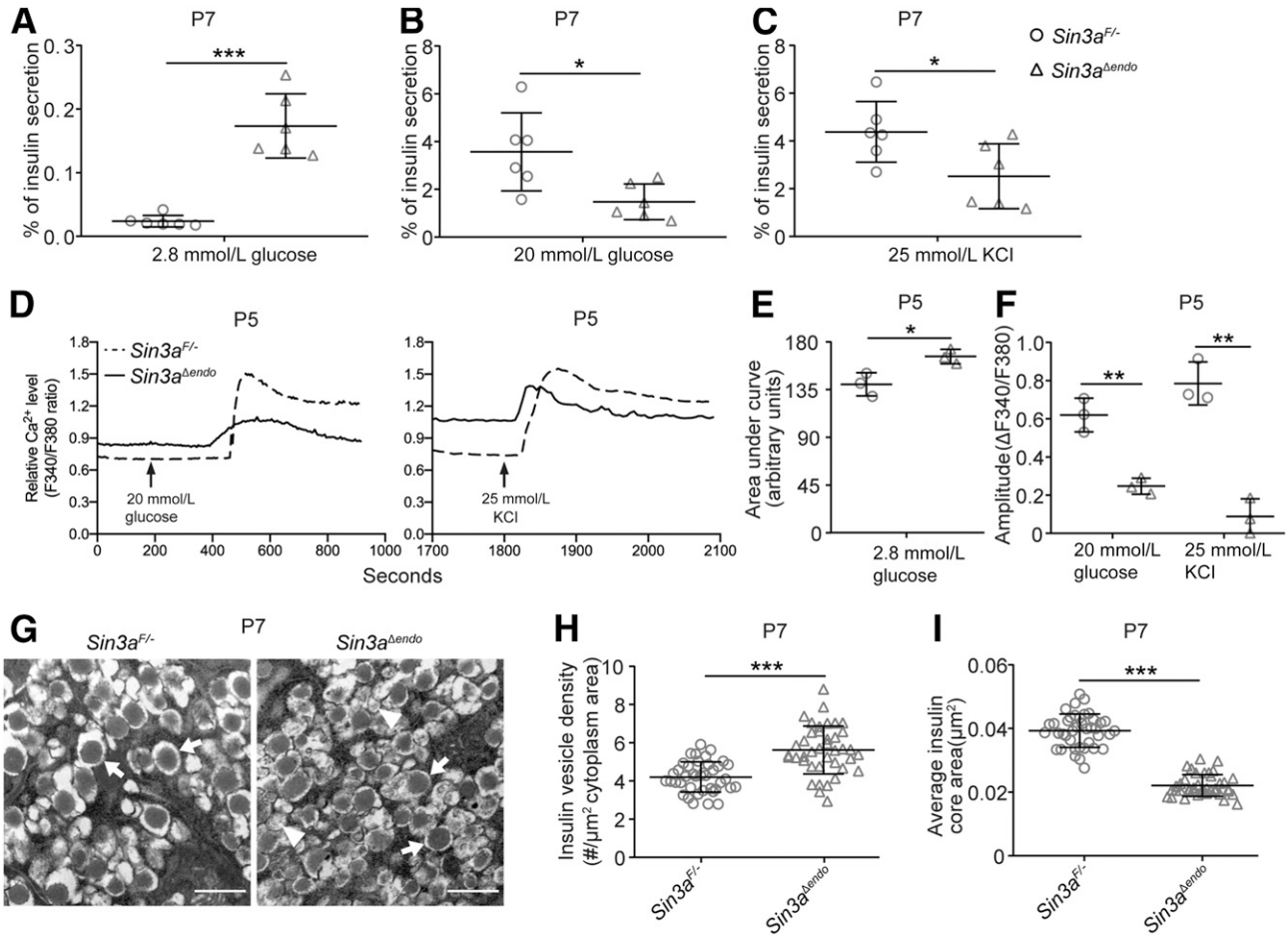

Figure 3—Sin3a promotes insulin secretion and granule biosynthesis. *A–C*: Insulin secretion in P7 $Sin3a^{F/-}$ control and $Sin3a^{\Delta endo}$ islets (n = 6), presented as % of insulin secretion within a 45-min window. *D–F*: Quantification of Ca^{2+} influx from P5 control and $Sin3a^{\Delta endo}$ islets, with representative Ca^{2+} recording (*D*), the overall Ca^{2+} influx at 2.8 mmol/L glucose (area under the curve 0–195 s) (*E*) and the highest Ca^{2+} influx amplitude at 20 mmol/L glucose and 25 mmol/L KCl stimulation (n = 3 mice) (*F*). *G*: TEM images of P7 β-cells. Arrows indicate normal insulin vesicles; arrowheads indicate empty vesicles. *H* and *I*: Vesicular quantification of P7 control and mutant β-cells (n = 40 images from two batches of mice), including vesicle density (*H*) and size (*I*). Scale bars = 500 nm. *$P < 0.05$, **$P < 0.01$, ***$P < 0.001$.

we comprehensively defined the Sin3a-regulated genes in β-cells by RNA-seq approaches.

Sin3a Regulates Genes Involved in Ion Transport, Cell Death, Vesicular Production/Secretion, Glucose Metabolism, and Stress Response

scRNA-seq was used to examine gene expression of P4 control and $Sin3a^{\Delta endo}$ islets, allowing us to distinguish β-cells from other islet cell types. P4 $Sin3a^{\Delta endo}$ mice had no recognizable physiological defects, avoiding complications imposed by hyperglycemia, but had increased β-cell death, underscoring the existing molecular defects in the P4 $Sin3a^{\Delta endo}$ β-cells.

Two highly reiterative scRNA-seq data sets (Fig. 6*A*) were obtained, which showed clear islet cell type separations (Supplementary Fig. 5). Differences in expression were seen between control and $Sin3a^{\Delta endo}$ β-cells, with both downregulated and upregulated genes (e.g., *Ucn3* that recapitulates qRT-PCR results, *Hspe1* that represents newly identified Sin3a-regulated genes, respectively) (Fig. 6*B*).

To minimize the saturation and scarcity issues inherent to scRNA-seq (31), we analyzed the scRNA-seq results by combining identical cell types into bulk expression data within each sample (32). This revealed 772 downregulated and 3,668 upregulated genes in $Sin3a^{\Delta endo}$ β-cells, with adjusted $P <$ 0.05 and at least a onefold increase or difference in expression (i.e., the expression level in one sample is at least twice as much as the other; see the table "Sin3 candidate gene list.xlsm" in GEO [GSE146474]). We observed the changed transcript level of *Ucn3* but not *Mafa*, *Nkx6.1*, *or Pdx1*, consistent with IF (Supplementary Fig. 3) and qRT-PCR results (Fig. 5*P*). GSEA of the scRNA-seq data set revealed several altered molecular pathways (Fig. 6*C*). The terms include protein/membrane transport/endoplasmic reticulum function, tricarboxylic acid cycle/mitochondrial activities, and oxidative stress responses.

Sin3a Is Enriched in 5′ Regulatory Regions of Several β-Cell Function/Survival Genes

Sin3a was reported to associate with several widely expressed DNA-binding proteins, including P53, Myc, Mad1,

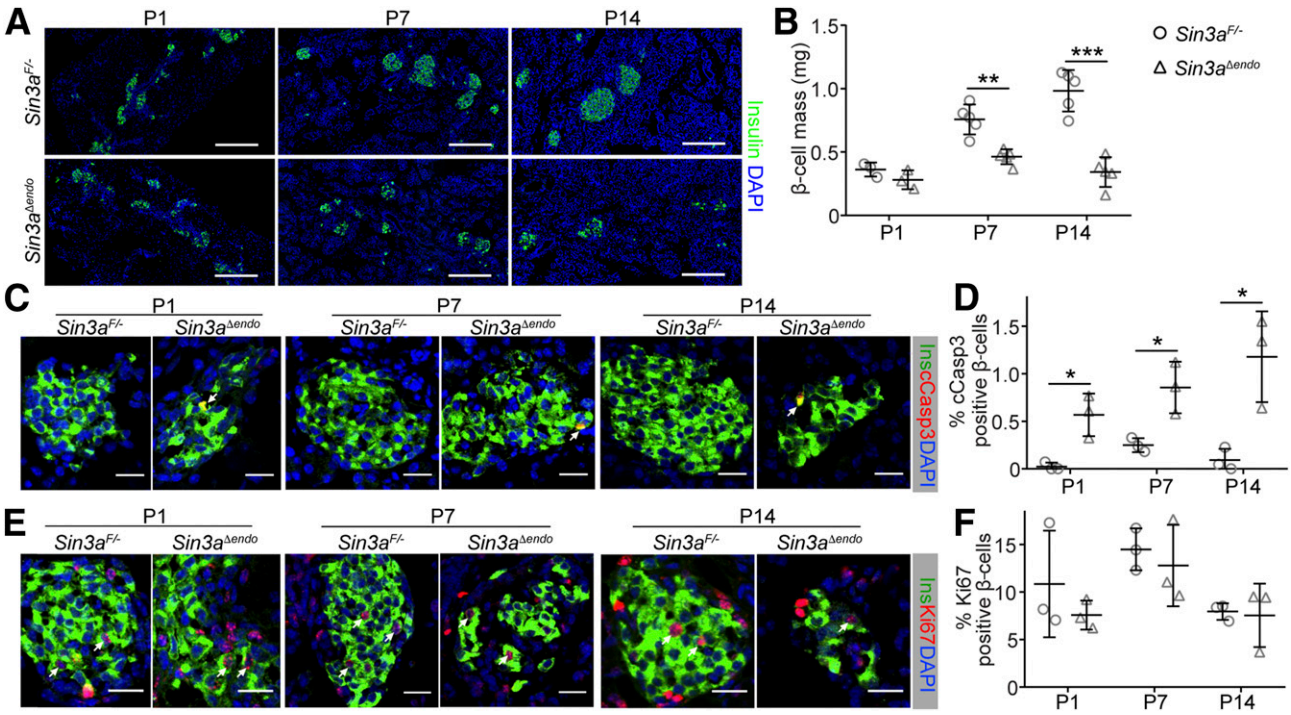

Figure 4— Sin3a is required for postnatal β-cell survival. *A* and *B*: Quantification of β-cell mass using IF assays ($n = 3$–5). Scale bar = 200 μm. *C*–*F*: Co-IF staining of insulin with cleaved caspase-3 (cCasp3) or Ki67 and the quantification ($n = 3$). Arrows in *E* indicate cCasp3$^+$ (*C*) or Ki67$^+$ β-cells. Scale bars = 20 μm. *$P < 0.05$, **$P < 0.01$, ***$P < 0.001$.

and Foxo1 (20,33). Sin3a was also detected in a Mafa-containing transcriptional complex, highly expressed in islet β-cells (3). We postulated that Sin3a shares common target genes among different cell types. Bioinformatics analyses were used to identify putative Sin3 target genes in β-cells by comparing the list of Sin3a-dependent genes with published Sin3a-based chromatin immunoprecipitation sequencing (ChIP-seq) results in mouse ES cells (34), epiblast stem cells (35), and muscle cells (13). We also included the Mafa-bound enhancers in mouse islets, postulating that the Sin3a associates with these sites through Mafa (35,36). This analysis revealed 2,847 gene loci having at least one reported Sin3a/Mafa-binding site, with 335 being downregulated and 2,512 being upregulated in *Sin3a*$^{\Delta endo}$ β-cells (see the table "Sin3 candidate gene list.xlsm" in GEO [GSE146474]). Gene ontology–based analyses (Database for Annotation, Visualization, and Integrated Discovery) revealed that these Sin3a-associated genes likely regulate processes in mitochondrion, endoplasmic reticulum/protein transport, ribosome, cell redox homeostasis, and synapses (Fig. 6*C* and *D*), similar to pathways revealed by GSEA analysis of all differentially expressed genes.

ChIP-PCR was used to verify whether some of these predicted genes are direct targets of Sin3a in MIN6 β-cells. We prioritized several genes that have established molecular functions that correlated with the cellular defects of *Sin3a*$^{\Delta endo}$ β-cells (Table 1). These include downregulated *Ins1* and *Kcnh2* required for insulin production and cell membrane polarization (37). They also include upregulated genes *Esyt1* and *Calr* (related to defective Ca^{2+} homeostasis) (38,39); *Bnip3*, *Casp3*, and *Ing1* (cell death) (40,41); *Arl6*, *Cltb*, *Ergic3*, and *Rab11a* (lipid transport and vesicular biosynthesis) (42–45); *Aldoa* and *Idh3a* (glucose metabolism); and *Hsp90b1* and *Hspe1* (stress responses) (46). *Mafa* was also included because Sin3a enrichment was detected on its putative regulatory elements (Table1). *Ucn3*, *Slc2a2*, *Gcg*, *Gapdh*, and albumin were included as controls because Sin3a was not reported to directly regulate these genes (Fig. 6*E* and Supplementary Fig. 6).

For ChIP-PCR, we selected several putative regulatory regions (RRs) in the 5′ region of each gene with putative Myc/P53-binding sites (47) (Supplementary Table 1). We found significantly enriched Sin3a occupancy in the 5′ RRs of *Kcnh2*, *Esyt1*, *Bnip3*, *Casp3*, *Ing1*, *Cltb*, *Rab11a*, *Aldoa*, *Hsp90b1*, and *Hspe1* (Fig. 7*A*). Corresponding to these results, qRT-PCR assays detected significantly decreased transcription of *Kcnh2* but increased expression of *Bnip3*, *Casp3*, *Ing1*, *Rab11a*, *Aldoa*, and *Hspe1* in P4 *Sin3a*$^{\Delta endo}$ islets, matching the scRNA-seq results (Fig. 7*B* and Table 1). We did not detect Sin3a enrichment in the tested regions of *Ins1*, *Gcg*, *Calr*, *Arl6*, *Ergic3*, and *Ucn3* genes (Supplementary Fig. 6). Intriguingly, we also found enriched Sin3a binding to the 5′ regions of *Slc2a2* and *Mafa*, although their expression levels remain unchanged in P4 *Sin3a*$^{\Delta endo}$ β-cells (Table 1). It is not clear whether Sin3a directly regulates these two genes in older β-cells.

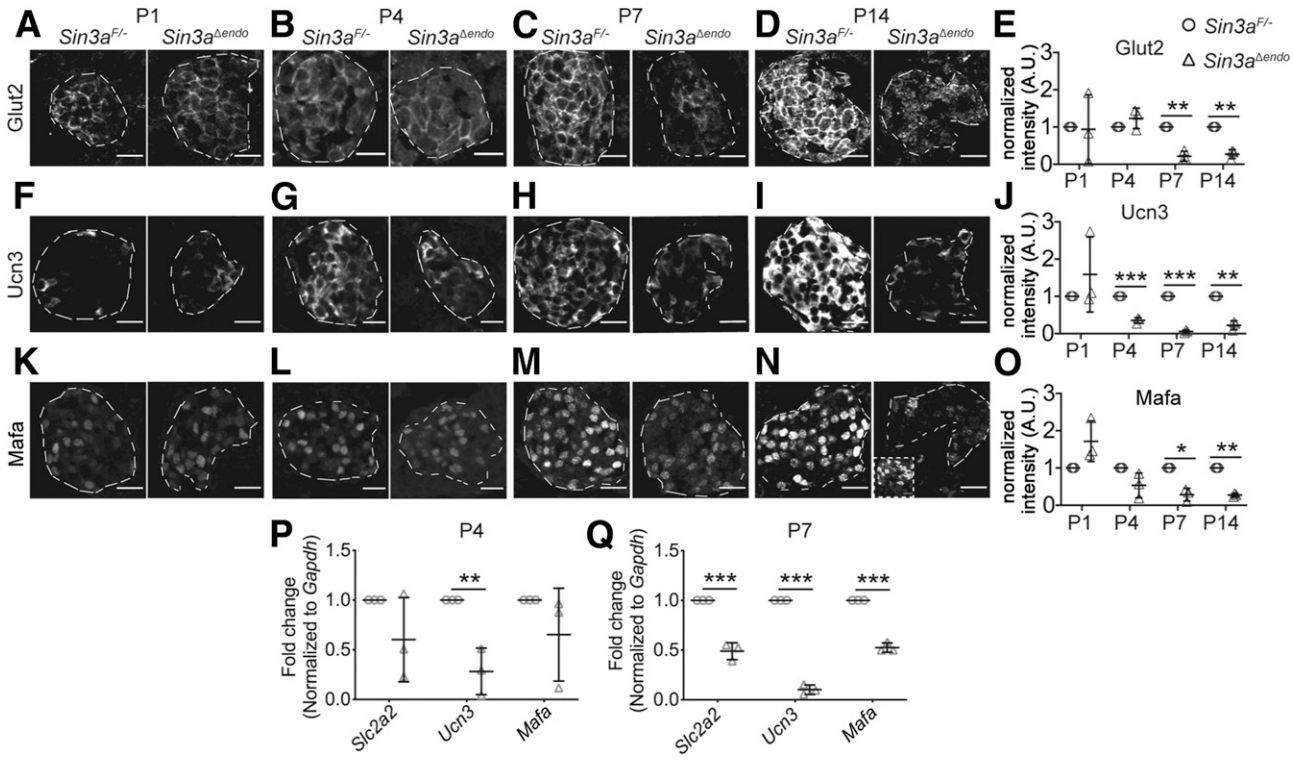

Figure 5— Postnatal *Sin3a*-deficient β-cells lack the expression of several functional genes. *A–E*: Glut2 staining and quantification in islets of different ages with or without *Sin3a* inactivation. *F–J* and *K–O*: The same as above expect Ucn3 and Mafa protein levels were measured, respectively ($n = 3$ mice for all assays). Scale bars = 20 μm. Broken lines encircle the islet areas, highlighting the signal intensity. Refer to the insulin IF in Supplementary Fig. 4 to see how β-cells were located. Inset in *N* shows an example of corresponding insulin signals. *P* and *Q*: Relative expression of *Slc2a2* (encoding Glut2), *Ucn3*, and *Mafa* in P4 and P7 islets, assayed using qRT-PCR. The gene expression levels were normalized to *Gapdh* ($n = 3$ mice). $^*P < 0.05$, $^{**}P < 0.01$, $^{***}P < 0.001$. A.U., arbitrary unit.

Sin3a and Sin3b Are Required for Endocrine Cell Specification

An intriguing finding is the upregulation of *Sin3b* in the absence of *Sin3a* (Table 1). We therefore tested whether inactivating *Sin3b* could further exacerbate the defects in $Sin3a^{\Delta endo}$ β-cells. Inactivating *Sin3b* alone in $Sin3b^{F/-}$; *Neurog3-Cre* mice produced no detectable phenotypes (data not shown), yet $Sin3a^{F/-}$; $Sin3b^{F/-}$; *Neurog3-Cre* ($Sin3a/3b^{\Delta endo}$) mice became diabetic before P5, at least 1 week earlier than $Sin3a^{\Delta endo}$ mice (Supplementary Fig. 7*A*), accompanied by largely reduced β-cell production (Supplementary Fig. 7*B*). These findings support the redundant function of *Sin3a* and *Sin3b* for the production/survival of islet β-cells.

Finally, we tested the roles of *Sin3a* and *Sin3b* in the pancreatic MPCs. $Sin3a^{F/F}$; $Sin3b^{F/F}$; $Pdx1^{Cre}$ (yielding $Sin3a/3b^{\Delta Panc}$ mice), and $Sin3a^{F/F}$; $Sin3b^{F/F}$; $Pdx1^{Cre}$; *Ai9* mice were derived. The *Ai9* Cre-reporter allele in the latter marked *Sin3a/Sin3b*-deficient pancreatic cells with tdTomato (23). At E15.5 and P1, there was substantially reduced production of β- and α-cells in $Sin3a/3b^{\Delta Panc}$ pancreata (Supplementary Fig. 7*C–E*), accompanied by reduced $Neurog3^+$ cell production (E15.5) (Supplementary Fig. 7*F*) and increased β-cell death (P1) (Supplementary Fig. 7*G*). Notably, the majority of pancreatic cells in $Sin3a^{F/F}$; $Sin3b^{F/F}$; $Pdx1^{Cre}$; *Ai9* mice expressed tdTomato, suggesting that *Sin3a/3b*-deficient pancreatic cells do not die immediately after *Sin3* inactivation (Supplementary Fig. 7*H*).

DISCUSSION

The mammalian Sin3a and Sin3b paralogs are scaffold proteins for the overall Sin3 coregulator complex that can associate with common TFs, such as Foxo, Mad1, Myc, and P53, and β-cell TFs Mafa and Myt (3). These associations recruit histone deacetylases, histone lysine methylases, and demethylase to regulate gene transcription in a highly cell context–dependent manner (5). We report here that inactivating *Sin3a* singly in the early mouse pancreatic endocrine lineage has little effect on islet cell differentiation but substantially reduces postnatal β-cell fitness without affecting the survival of δ-cells. The *Sin3a*-deficient β-cells showed defective insulin secretion, cell survival, Ca^{2+} influx, and insulin vesicle biogenesis. We further showed that Sin3a associates with putative enhancers of several genes involved in ion transport/Ca^{2+} homeostasis, cell death, membrane trafficking, glucose metabolism, and stress response in β-cells. Intriguingly, inactivating both *Sin3a* and *Sin3b* in the same endocrine lineage resulted in further reduction of endocrine cell numbers by birth, while coinactivating both *Sin3a* and *Sin3b* in the early pancreatic MPCs substantially

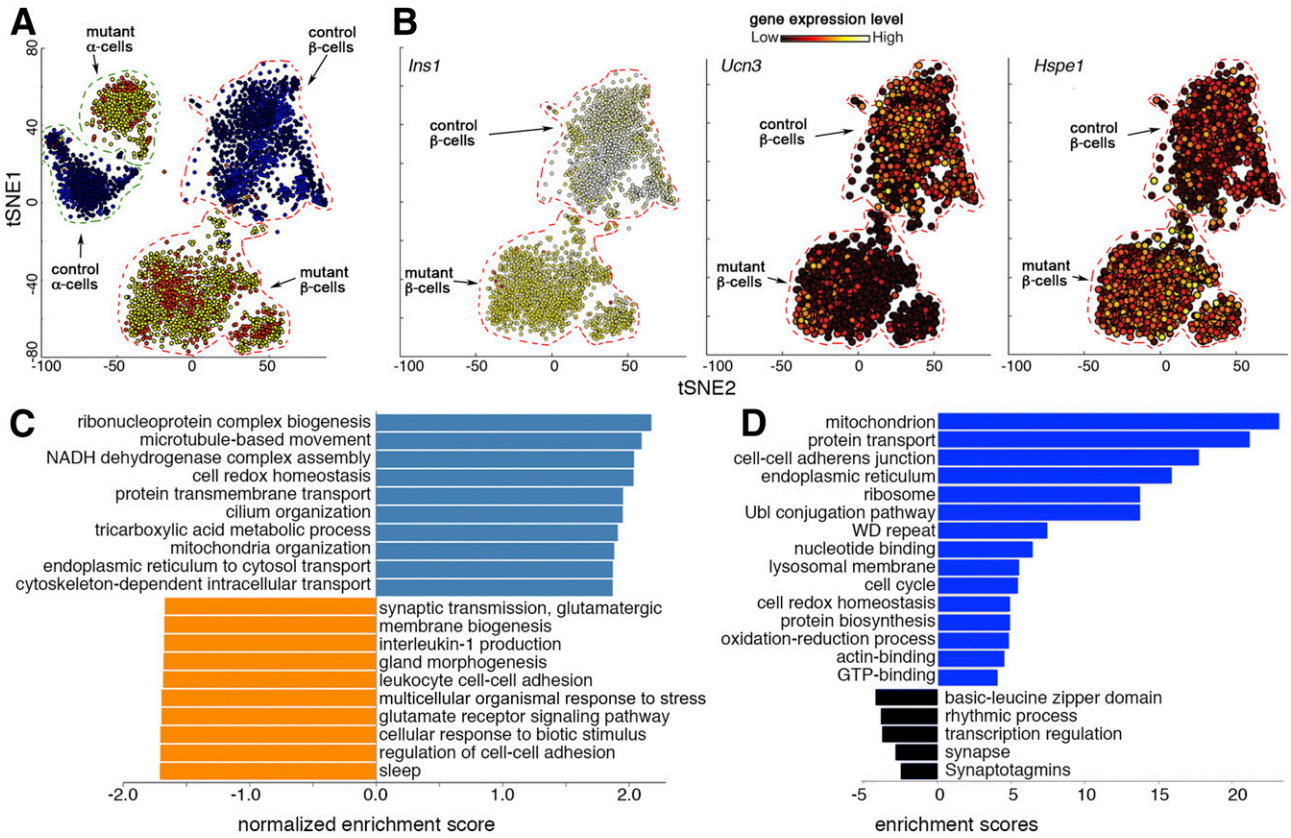

Figure 6—scRNA-seq identifies Sin3a-dependent genes and pathways in islet β-cells. *A*: t-Distributed stochastic neighbor embedding (tSNE)–aided visualization of α-cell (green circles) and β-cell (red circles) clusters in two duplicate experiments, with both control and *Sin3a*$^{\Delta endo}$-mutant cells. Note that cells from each experiment are represented by dots of different colors (black and blue for control samples, red and yellow for mutant cells). *B*: The expression of *Ins1*, *Ucn3*, and *Hspe1* in β-cells on the tSNE map. Note that in this panel, the color of dots indicates the relative gene expression level, with white indicating the highest expression level and black the lowest expression level. *C*: GSEA results of all differentially expressed genes in control and *Sin3a*$^{\Delta endo}$ β-cells. Pathways with false discovery rate ≤0.05 are shown. *D*: Gene ontology clustering of differentially expressed genes that were also reported to be direct Sin3a targets in several cell types. Only the top 15 upregulated terms (enrichment score >4.8) and top 5 downregulated terms (enrichment score >2.4) are listed.

reduced production of endocrine progenitors without preventing their differentiation into hormone-positive islet cells.

Our discoveries highlight a few features of Sin3 function in pancreatic cells. First, although *Sin3a* but not *Sin3b* is required for producing postnatal β-cells with similar "fitness qualities," both paralogs can prevent cell death. Thus, inactivating *Sin3b* expedited islet cell loss in *Sin3a*-null islets. It is possible that Sin3a and Sin3b regulate a similar set of molecular targets, yet Sin3a contributes a higher proportion of such activity because of a higher affinity for transcriptional effectors. Alternatively, Sin3a and Sin3b may regulate different sets of target genes that have similar functions. Future comparisons of transcriptomic alterations between *Sin3a*-null and *Sin3b*-null β-cells together with comprehensive ChIP-seq analyses should address these possibilities. In either case, it appears that the total Sin3 activity has to achieve a certain threshold to maintain normal β-cell fitness.

The second feature is that different islet cell types have different levels of Sin3a dependency, with α- and β-cells, but not δ-cells, requiring Sin3a for postnatal survival. It is possible that Sin3a regulates similar gene sets in all islet cell types but that the cellular context dictates resistance to cell death pathways. Alternatively, different islet cell types may use different Sin3a-TF complexes to regulate transcription. Follow-up identification of these complexes using proteomic studies could address this question.

Third, although Sin3 (either Sin3a or Sin3b) is required in MPCs to promote endocrine specification, their overall activities are dispensable for the differentiation of committed endocrine progenitors into hormone-expressing islet cells. Therefore, our collective findings, combined with Sin3a's reported roles in the differentiation of several nonpancreatic cells (13–15,17,48), highlight the idea that pancreatic cells use the Sin3-TF complexes differentially in a stage- and/or cell type–specific manner for differentiation, function, and survival.

The compromised β-cell fitness in *Sin3a*-null mice is consistent with Sin3a being a coregulator recruited by Mafa and Foxo1, both of which interact with Sin3a and are essential for β-cell fitness (20,49). However, *Sin3a*-null

Table 1—Several candidate genes studied by ChIP-PCR and qRT-PCR assays

Function category	Gene	LogFC	Percentage of mutant	Percentage of control	Adjusted *P* value	Sin3a binding				Mafa site
						Epiblast (35)	ES Ab1* (34)	ES Ab2* (34)	Muscle (13)	Islets (36)
Hormone	*Ins1*	−0.838	0.998	1.00	4.20E-120					Yes
Function/maturation	*Slc2a2*	−0.002	0.911	0.843	1.00					
	Mafa	−0.007	0.002	0.005	1.00	Yes	Yes		Yes	
	Ucn3	−1.041	0.373	0.715	1.65E-106					
	Pdx1	−0.143	0.531	0.544	1.00					
Channel	*Kcnh2*	−0.728	0.394	0.541	8.89E-40	Yes	Yes	Yes		
Ca^{2+} homeostasis	*Esyt1*	0.588	0.764	0.355	4.10E-133		Yes	Yes		
	Calr	0.344	0.985	0.923	3.09E-70		Yes	Yes		
Cell death	*Bnip3*	0.572	0.777	0.363	1.32E-113		Yes			
	Casp3	0.617	0.723	0.277	1.89E-131		Yes			
	Ing1	0.683	0.770	0.332	3.65E-140		Yes		Yes	
Lipid transport	*Arl1*	0.324	0.397	0.125	2.32E-57	Yes	Yes	Yes		
	Cltb	0.346	0.854	0.608	3.02E-55		Yes	Yes		
	Ergic3	0.335	0.760	0.491	8.56E-48		Yes	Yes	Yes	
	Rab11a	0.324	0.790	0.522	7.11E-49		Yes	Yes		
Metabolism	*Aldoa*	0.609	0.757	0.368	5.93E-123	Yes	Yes	Yes		
	Idh3a	0.542	0.794	0.318	1.59E-105		Yes	Yes	Yes	
Stress response	*Hsp90b1*	0.596	0.982	0.883	9.66E-171			Yes	Yes	
	Hspe1	0.709	0.885	0.552	3.48E-151		Yes	Yes		
Paralog	*Sin3b*	0.198	0.437	0.225	2.85E-33					

Shown are the reported function, logFC of mutant over control β-cells, percentage of mutant and control β-cells that expressed each gene, and adjusted *P* values. Also indicated are whether Sin3a or Mafa was enriched in putative *cis*-RRs of each gene, from published data. Ab, antibody. *The data were from a single publication, with two Abs used for ChIP-seq.

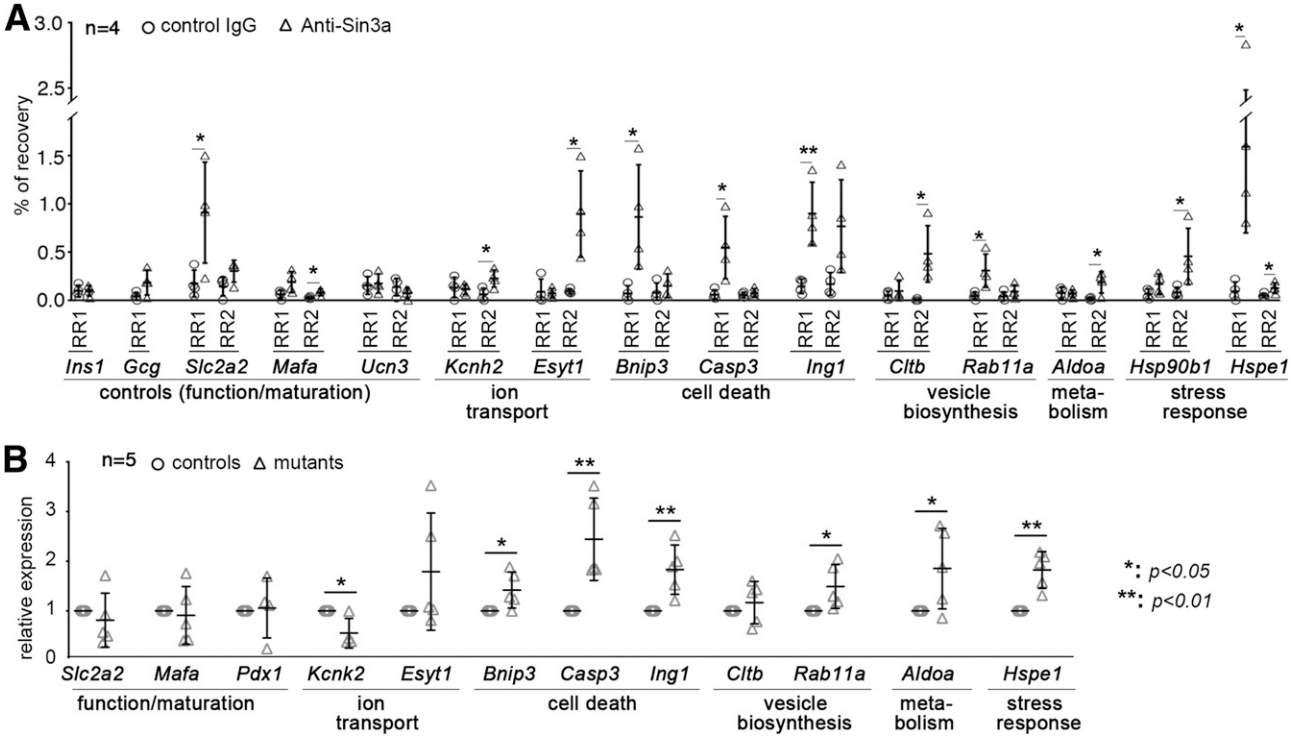

Figure 7—ChIP-PCR reveals several potential Sin3a target genes in MIN6 β-cells. *A*: ChIP-PCR assays of Sin3a-associated DNA RRs of several genes. Percentage of chromatin recovery is shown ($n = 4$ batches of chromatin preparations). Results of two RRs for each gene are presented. Normal IgG was used as control. The selected genes were grouped according to their reported functions (see text). *B*: qRT-PCR assays of gene transcription in P4 islets ($n = 5$ batches of islets, including 1–3 individual mice for each batch). The results were normalized against that of *Gapdh*. We then artificially set the relative expression level in control islets to 1.0 for comparison.

mice developed overt diabetes before weaning, while *Mafa*- and *Foxo1*-deficient mice only did so a significant period afterward. An implication is that *Sin3a* inactivation may be equivalent to coinactivation of *Mafa* and *Foxo1*. Alternatively, Sin3a may also mediate the function of additional TFs required for β-cell function and/or survival (e.g., Myc and P53), which are ubiquitous in most cell types. Our ChIP-PCR assays detected Sin3a enrichment in putative Myc/P53-binding enhancers of several genes in β-cells whose products regulate cell death, ion transport, lipid trafficking/vesicular biosynthesis, metabolism, and stress responses (Table 1). Thus, our collective findings are consistent with the idea that Myc/P53 could recruit Sin3a in β-cells to promote β-cell fitness by ensuring insulin vesicle biosynthesis, stimulus secretion coupling, and survival. Note that the complete list of key Sin3a/Sin3b targets in β-cells remains unknown. Future genome-wide ChIP-seq studies of β-cells using specific Sin3a and Sin3b antibodies, combined with transcriptomic analysis of the few *Sin3a/3b*$^{\Delta Endo}$ and/or *Sin3a/3b*$^{\Delta Panc}$ β-cells that are formed, may shed more light on how Sin3a and Sin3b regulate β-cells.

Sin3 has been functionally diagnosed as both a coactivator and a corepressor. Consistent with this notion, we found both downregulated and upregulated genes in *Sin3a*-deficient β-cells, with many being reported as directly regulated by Sin3a in other cell types. Our candidate ChIP-PCR assays corroborated enrichment of Sin3a in putative regulatory regions of Sin3-repressed (e.g., *Hspe1*, *Casp3*) and -activated genes (*Kcnh2*) in β-cells, underscoring the bi-directional regulatory roles of Sin3a.

In summary, our findings show that the Sin3 coregulator plays essential roles in islet-cell production and postnatal β-cell fitness, with Sin3a being the major contributor. Thus, modulating Sin3a levels or activities could be explored to protect β-cell fitness and to control diabetes initiation and progression.

Acknowledgments. The authors thank Dr. Roland Stein (Vanderbilt University) for useful discussions about the Sin3 activities, Drs. Chin Chiang and Lei Chen (Vanderbilt University) for help with ChIP-PCR, and William Gu (Montgomery Bell Academy, Nashville, TN) for text editing.

Funding. This study is supported by grants from the National Institute of Diabetes and Digestive and Kidney Diseases (DK-106228 to I.K. and G.G., DK-103831 and CA-095103 to K.S.L., and DK-065949 to G.G.) and JDRF (1-2009-371 to G.G.). Confocal and TEM imaging was performed with Vanderbilt University Cell Imaging Shared Resource (supported by National Institutes of Health [NIH] grants CA-68485, DK-20593, 500 DK-58404, DK-59637, and EY-08126). Vanderbilt University Medical Center Hormone Assay and Analytical Services Core was supported by NIH grants DK-059637 (Mouse Metabolic Phenotyping Center) and DK-020593 (Diabetes Research and Training Center) and the Islet Procurement & Analysis Core by DK-020593. DNA sequencing was done by Vanderbilt Technologies for Advanced Genomics, supported by the Vanderbilt Ingram Cancer Center (P30-CA-68485), the Vanderbilt Vision Center

(P30-EY-08126), and NIH/National Center for Research Resources (G20-RR-030956).

Duality of Interest. No potential conflicts of interest relevant to this article were reported.

Author Contributions. X.Y., S.M.G., K.-H.H., D.A.J., K.S.L., and G.G. analyzed data. X.Y., S.M.G., A.J.S., and G.G. performed the experiments. X.Y., D.A.J., I.K., C.V.E.W., K.S.L., and G.G. designed the experiments. X.Y., K.S.L., and G.G. prepared figures. C.N.H., B.C., A.N.S-S., and K.S.L. performed the scRNA-seq analysis. G.D. provided the mice harboring *Sin3a/Sin3b* floxed alleles. All authors helped with data interpretation, participated in manuscript writing/proofreading, and the approved final version of the manuscript. G.G. is the guarantor of this work and, as such, had full access to all the data in the study and takes responsibility for the integrity of the data and the accuracy of the data analysis.

Prior Presentation. Parts of this study were presented at the 11th Annual Midwest Islet Club, St. Louis, MO, 14-15 May 2018, and 12th Annual Midwest Islet Club, Ann Arbor, MI, 19–20 May 2019.

References

1. Larsen HL, Grapin-Botton A. The molecular and morphogenetic basis of pancreas organogenesis. Semin Cell Dev Biol 2017;66:51–68

2. Salinno C, Cota P, Bastidas-Ponce A, Tarquis-Medina M, Lickert H, Bakhti M. β-Cell maturation and identity in health and disease. Int J Mol Sci 2019;20:5471

3. Scoville DW, Cyphert HA, Liao L, et al. MLL3 and MLL4 methyltransferases bind to the MAFA and MAFB transcription factors to regulate islet β-cell function. Diabetes 2015;64:3772–3783

4. Spaeth JM, Walker EM, Stein R. Impact of Pdx1-associated chromatin modifiers on islet β-cells. Diabetes Obes Metab 2016;18(Suppl. 1):123–127

5. Kadamb R, Mittal S, Bansal N, Batra H, Saluja D. Sin3: insight into its transcription regulatory functions. Eur J Cell Biol 2013;92:237–246

6. Barnes VL, Laity KA, Pilecki M, Pile LA. Systematic analysis of SIN3 histone modifying complex components during development. Sci Rep 2018;8:17048

7. Yang Y, Huang W, Qiu R, et al. LSD1 coordinates with the SIN3A/HDAC complex and maintains sensitivity to chemotherapy in breast cancer. J Mol Cell Biol 2018;10:285–301

8. Zhu F, Zhu Q, Ye D, et al. Sin3a-Tet1 interaction activates gene transcription and is required for embryonic stem cell pluripotency. Nucleic Acids Res 2018;46:6026–6040

9. Liu M, Saha N, Gajan A, Saadat N, Gupta SV, Pile LA. A complex interplay between SAM synthetase and the epigenetic regulator SIN3 controls metabolism and transcription. J Biol Chem 2020;295:375–389

10. Chaubal A, Pile LA. Same agent, different messages: insight into transcriptional regulation by SIN3 isoforms. Epigenetics Chromatin 2018;11:17

11. Streubel G, Fitzpatrick DJ, Oliviero G, et al. Fam60a defines a variant Sin3a-Hdac complex in embryonic stem cells required for self-renewal. EMBO J 2017;36:2216–2232

12. Saunders A, Huang X, Fidalgo M, et al. The SIN3A/HDAC corepressor complex functionally cooperates with NANOG to promote pluripotency. Cell Rep 2017;18:1713–1726

13. van Oevelen C, Bowman C, Pellegrino J, et al. The mammalian Sin3 proteins are required for muscle development and sarcomere specification. Mol Cell Biol 2010;30:5686–5697

14. Pellegrino J, Castrillon DH, David G. Chromatin associated Sin3A is essential for male germ cell lineage in the mouse. Dev Biol 2012;369:349–355

15. Yao C, Carraro G, Konda B, et al. Sin3a regulates epithelial progenitor cell fate during lung development. Development 2017;144:2618–2628

16. Nascimento EM, Cox CL, MacArthur S, et al. The opposing transcriptional functions of Sin3a and c-Myc are required to maintain tissue homeostasis. Nat Cell Biol 2011;13:1395–1405

17. Dannenberg JH, David G, Zhong S, van der Torre J, Wong WH, Depinho RA. mSin3A corepressor regulates diverse transcriptional networks governing normal and neoplastic growth and survival. Genes Dev 2005;19:1581–1595

18. Tiana M, Acosta-Iborra B, Puente-Santamaría L, et al. The SIN3A histone deacetylase complex is required for a complete transcriptional response to hypoxia. Nucleic Acids Res 2018;46:120–133

19. Huang C, Walker EM, Dadi PK, et al. Synaptotagmin 4 regulates pancreatic β cell maturation by modulating the Ca^{2+} sensitivity of insulin secretion vesicles. Dev Cell 2018;45:347–361.e5

20. Langlet F, Haeusler RA, Linden D, et al. Selective inhibition of FOXO1 activator/repressor balance modulates hepatic glucose handling. Cell 2017;171:824–835.e18

21. David G, Grandinetti KB, Finnerty PM, Simpson N, Chu GC, Depinho RA. Specific requirement of the chromatin modifier mSin3B in cell cycle exit and cellular differentiation. Proc Natl Acad Sci U S A 2008;105:4168–4172

22. Pan FC, Brissova M, Powers AC, Pfaff S, Wright CV. Inactivating the permanent neonatal diabetes gene Mnx1 switches insulin-producing β-cells to a δ-like fate and reveals a facultative proliferative capacity in aged β-cells. Development 2015;142:3637–3648

23. Liu J, Banerjee A, Herring CA, et al. Neurog3-Independent methylation is the earliest detectable mark distinguishing pancreatic progenitor identity. Dev Cell 2019;48:49–63.e7

24. Jacobson DA, Mendez F, Thompson M, Torres J, Cochet O, Philipson LH. Calcium-activated and voltage-gated potassium channels of the pancreatic islet impart distinct and complementary roles during secretagogue induced electrical responses. J Physiol 2010;588:3525–3537

25. Tabula Muris Consortium; Overall Coordination; Logistical Coordination; Organ Collection and Processing; Library Preparation and Sequencing; Computational Data Analysis; Cell Type Annotation; Writing Group; Supplemental Text Writing Group; Principal Investigators. Single-cell transcriptomics of 20 mouse organs creates a Tabula Muris. Nature 2018;562:367–372

26. Subramanian A, Tamayo P, Mootha VK, et al. Gene set enrichment analysis: a knowledge-based approach for interpreting genome-wide expression profiles. Proc Natl Acad Sci U S A 2005;102:15545–15550

27. Huang W, Sherman BT, Lempicki RA. Systematic and integrative analysis of large gene lists using DAVID bioinformatics resources. Nat Protoc 2009;4:44–57

28. Magnuson MA, Osipovich AB. Pancreas-specific Cre driver lines and considerations for their prudent use. Cell Metab 2013;18:9–20

29. Li C, Chen P, Vaughan J, Lee KF, Vale W. Urocortin 3 regulates glucose-stimulated insulin secretion and energy homeostasis. Proc Natl Acad Sci U S A 2007;104:4206–4211

30. Hang Y, Stein R. MafA and MafB activity in pancreatic β cells. Trends Endocrinol Metab 2011;22:364–373

31. Mawla AM, Huising MO. Navigating the depths and avoiding the shallows of pancreatic islet cell transcriptomes. Diabetes 2019;68:1380–1393

32. Svensson V, Natarajan KN, Ly LH, et al. Power analysis of single-cell RNA-sequencing experiments. Nat Methods 2017;14:381–387

33. Bansal N, David G, Farias E, Waxman S. Emerging roles of epigenetic regulator Sin3 in cancer. Adv Cancer Res 2016;130:113–135

34. Williams K, Christensen J, Pedersen MT, et al. TET1 and hydroxymethylcytosine in transcription and DNA methylation fidelity. Nature 2011;473:343–348

35. Seki M, Masaki H, Arauchi T, Nakauchi H, Sugano S, Suzuki Y. A comparison of the rest complex binding patterns in embryonic stem cells and epiblast stem cells. PLoS One 2014;9:e95374

36. Tennant BR, Robertson AG, Kramer M, et al. Identification and analysis of murine pancreatic islet enhancers. Diabetologia 2013;56:542–552

37. Hardy AB, Fox JE, Giglou PR, et al. Characterization of Erg K+ channels in alpha- and beta-cells of mouse and human islets. J Biol Chem 2009;284:30441–30452

38. Yu H, Liu Y, Gulbranson DR, Paine A, Rathore SS, Shen J. Extended synaptotagmins are Ca2+-dependent lipid transfer proteins at membrane contact sites. Proc Natl Acad Sci U S A 2016;113:4362–4367

39. Wang WA, Liu WX, Durnaoglu S, et al. Loss of calreticulin uncovers a critical role for calcium in regulating cellular lipid homeostasis. Sci Rep 2017;7:5941

40. Bose P, Thakur S, Thalappilly S, et al. ING1 induces apoptosis through direct effects at the mitochondria. Cell Death Dis 2013;4:e788
41. Ma Z, Chen C, Tang P, Zhang H, Yue J, Yu Z. BNIP3 induces apoptosis and protective autophagy under hypoxia in esophageal squamous cell carcinoma cell lines: BNIP3 regulates cell death. Dis Esophagus 2017;30:1–8
42. Price HP, Hodgkinson MR, Wright MH, et al. A role for the vesicle-associated tubulin binding protein ARL6 (BBS3) in flagellum extension in Trypanosoma brucei. Biochim Biophys Acta 2012;1823:1178–1191
43. Pearse BM. Clathrin: a unique protein associated with intracellular transfer of membrane by coated vesicles. Proc Natl Acad Sci U S A 1976;73:1255–1259
44. Sato K, Nakano A. Mechanisms of COPII vesicle formation and protein sorting. FEBS Lett 2007;581:2076–2082
45. Zhu S, Bhat S, Syan S, Kuchitsu Y, Fukuda M, Zurzolo C. Rab11a-Rab8a cascade regulates the formation of tunneling nanotubes through vesicle recycling. J Cell Sci 2018;131:jcs215889
46. Kim DS, Song L, Wang J, et al. GRP94 is an essential regulator of pancreatic β-cell development, mass, and function in male mice. Endocrinology 2018;159:1062–1073
47. Messeguer X, Escudero R, Farré D, Núñez O, Martínez J, Albà MM. PROMO: detection of known transcription regulatory elements using species-tailored searches. Bioinformatics 2002;18:333–334
48. Cowley SM, Iritani BM, Mendrysa SM, et al. The mSin3A chromatin-modifying complex is essential for embryogenesis and T-cell development. Mol Cell Biol 2005;25:6990–7004
49. Hang Y, Yamamoto T, Benninger RK, et al. The MafA transcription factor becomes essential to islet β-cells soon after birth. Diabetes 2014;63:1994–2005